

## Aero-Thermal Performance of Purge Flow in Turbine Cascade Endwall Cooling

W Ghopa Wan Aizon<sup>1,2,a</sup>, Ken-ichi Funazaki<sup>1,b</sup>

<sup>1</sup> Department of Mechanical Engineering, Iwate University, Morioka 020-8551 Iwate, Japan

<sup>2</sup> Department of Mechanical and Materials, National University of Malaysia, Bangi, Malaysia

<sup>a</sup>wanaizon@gmail.com, <sup>b</sup>funazaki@iwate-u.ac.jp

**Keywords:** endwall film cooling, purge flow, upstream leakage, secondary flow field, heat transfer

**Abstract.** The endwall and blade film cooling systems are the typical solution adopted within gas turbines to allow further increase of *turbine* inlet temperature, avoiding critical material thermal stresses. Due to complex secondary flow field in the blade passage, endwall is more difficult to cool than blade surfaces. In the matter of fact, in endwall film cooling studies, it is necessary to investigate the interaction between coolant air and the secondary flow. In present study, the flow field of high-pressure turbine cascade has been investigated by 5-holes pitot tube to reveal the secondary flows behavior under the influenced of purge flows while the heat transfer measurement was conducted by *thermochromic liquid crystal* (TLC). Experimental has significantly captured the aerodynamics effect of purge flow at blade downstream close to the endwall region. Furthermore, TLC measurement illustrated that the film cooling effectiveness and heat transfer coefficient contours were strongly influenced by the secondary flow on the endwall.

### Nomenclature

$C_{ax}$  : blade axial chord  
 $Q$  : volume flow rate  
 $U_{in}$  : inlet velocity  
 $\rho$  : density  
 $P_{ti}, P_{to}$  : inlet total pressure, outlet total pressure  
 $y/p$  : non-dimensional pitch direction  
 $z/s$  : non-dimensional span direction  
SS, PS : suction surface, pressure surface  
 $\infty, 2$  : main flow, secondary air  
MFR : mass flow ratio =  $(\rho Q)_2 / (\rho Q)_\infty$   
 $C_{pt}$  : total pressure loss coefficient =  $(P_{ti} - P_{to}) / ((1/2) \rho U_{in}^2)$   
 $\eta$  : film effectiveness  
 $h$  : heat transfer coefficient

### Introduction

Increasing the inlet temperature of gas turbines will improve their efficiency. Modern gas turbine are designed to operate at turbine inlet temperatures exceeding 1600 °C. Hence, it is essential to provide cooling components surfaces because of the extreme operating environment. In high pressure turbine nozzle, the endwall region is considerably more difficult to cool than the blade aerofoil surfaces because of the complex secondary flow structure in the blade passage. Blair[1] was the first to carried out the heat transfer investigation on the endwall. It is highlighted that the secondary flow structure plays a big role in dictating the endwall film cooling performance. The occurrence of horse-shoe vortex and the passage vortex swept the coolant towards the suction side corner leaving the pressure side unprotected. Acknowledging the important to understand the flow structure in the blade passage, numbers of research have done including the work of Langson [2], Takeshi et al[3] and Wang et al[4]. They found that due to the radial gradient in stagnation pressure at blade leading edge, two dimensional boundary layers entering the cascade roll up into a vortex

with a circumferential component of vorticity. This vortex then split into two legs of a horse-shoe vortex, with the suction side of the horse-shoe vortex follows the blade profile while the pressure side leg migrates from the pressure side to the next suction side due to the traversal pressure gradient and merges and becomes a part of the large passage vortex and flow downstream. Bypass leakage flow through the combustor-turbine endwall junction has been considered to be useful in providing a protective coolant layer prevented the endwall surface from the hot core flow coming from combustor side. The investigation about slot upstream leakage have been done by Kost and Nicklas[5] and Kost and Mullaert[6]. They stated that the ejection coolant from slot located at  $0.3C_{ax}$  stayed closer to the endwall and provided better cooling than slot located at  $0.2C_{ax}$  of cascade upstream. The slot placed close to the leading edge may increase the strength of the leading edge horse-shoe vortex. Recently, Papa et al.[7] had investigated the film cooling effect of purge flow on endwall and they found that due to the action of the passage vortex, a well-defined streak of cooling effectiveness on the blade suction surface also had been captured. In present works, the effects of the upstream leakage flow on the endwall cooling have been investigated in both thermal and also aerodynamic behavior. Realistic flow field which is similar to the flow in the HP turbine nozzle is reproduced using a linear cascade of the nozzle vanes combined with a secondary air supply system for injection of leakage air to the mainstream. The flow field measurements at blade downstream plane were performed by the use of Pneumatic 5-holes Pitot tube. Based on the data obtained, total pressure loss, secondary velocity vector and the flow vorticity were determined and discussed. Furthermore, this study took advantage of TLC to detect time-varying surface temperature on the endwall and the discussion about cooling effectiveness has been made.

### Aerodynamic Measurements

Fig. 1 (a) shows the top view of the test section consists of 2 segments, each of which had two identical HP turbine nozzle vanes, and two dummy vanes. The L-type miniature pitot tube was placed  $1.35C_{ax}$  upstream of blade leading edge for test condition setting. The secondary air was driven by a secondary blower and its flow rate was measured by the laminar flow-meter. Fig. 1 (b) indicates the upstream slot that mimicked the clearance between the HP turbine endwall and the combustion liner in real engines. The upstream slot was located  $0.24C_{ax}$  upstream of the vane leading edge. The slot extended to 4 pitches and the width was 4mm. The measurement system includes pneumatic 5-holes pitot tube, traverse device, pressure transducer and data logger which are connected to the computer for data recording. Since the measurements were for the aerodynamics purpose, the secondary air was supplied without any heating. As shown in Fig. 1 (a), S2 indicates the location of traverse slit which is located at  $0.5C_{ax}$  downstream of blade trailing edge. The main flow Reynolds number, was  $1.7 \times 10^5$  and determined based on actual blade chord were fixed throughout all test cases. The measurement without a leakage ejection was firstly carried out to observe a flow field of baseline condition at blade downstream plane. Furthermore, in order to study the effect of the upstream leakage ejection to the secondary flow field and the amount of leakage ejection as well, secondary air was ejected to the main stream approximately 1.0%, 1.5% and 2.0% of MFR, respectively. The probe was traversed for single pitch in pitchwise direction starting from midspan and ended at 2mm from the blade endwall. For each measuring point 10 samples have been collected and the pressures were calculated as time-averaged components. Fig. 1(a) also indicates the viewpoint definition of all contours presented in Fig. 2.

### Heat Transfer Measurement

In present study, transient methods based on Funazaki [8] were used to investigate the film cooling and heat transfer performance of leakage flow. For this purpose, the data such as time-varying temperature of the surface, secondary air temperature rise and initial temperature of test model surface need to be measured. TLC was used to detect time-varying surface temperature on the endwall. The TLC used in the present study was the commercial product (Nihon Capsule Products) and the color range was from  $25.5^\circ\text{C}$  to  $30.5^\circ\text{C}$ . The same MFR of leakage flow which

were used in aerodynamics study were tested. Fig. 1(c) shows the measurement system, including camera and light positions. The measurements were conducted by using the same test model used in the aerodynamics measurement. However, the test model was black painted in order to prevent the light reflection during the measurement. The color change of the TLC was recorded with digital video cameras, and recorded image data were captured by PC frame by frame, and then converted from RGB (Red/Green/Blue) images into HSL (Hue/Saturation/Lightness) images. Then, the relation between Hue and temperature obtained from the calibration of TLC were used to determine the adiabatic wall temperature of endwall surface.

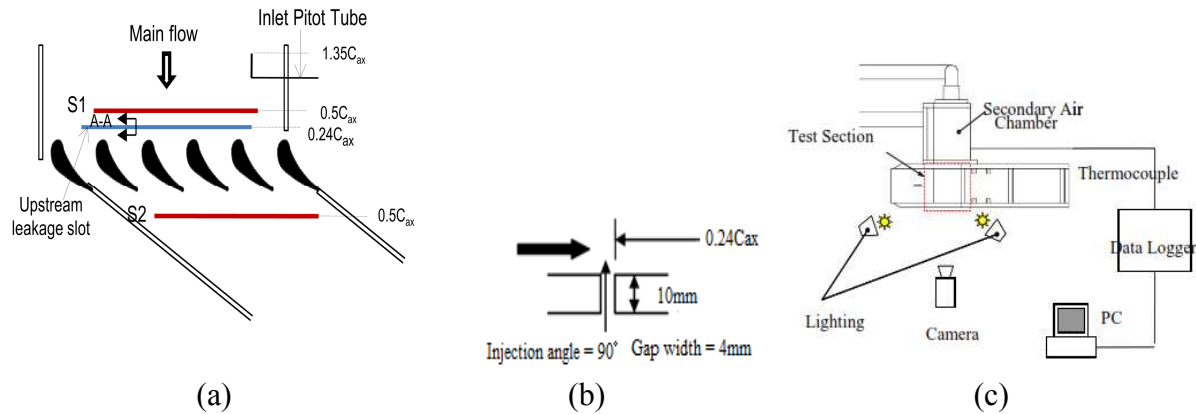
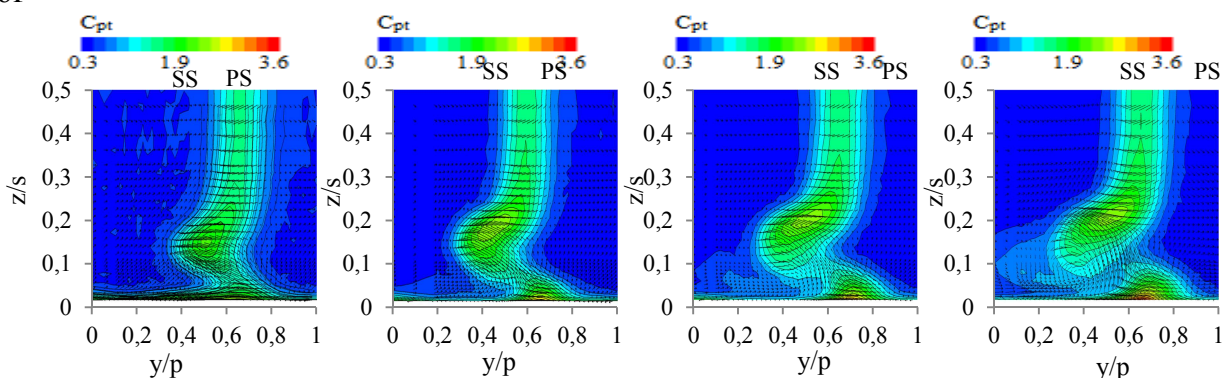


Fig. 1 Experimental setup for aerodynamic and heat transfer

## Results and Discussions

**Aerodynamics Performance.** Fig. 2 demonstrates contours of total pressure loss (top figure) with secondary velocity vector map superimposed while the bottom one shows the vorticity at the same plane. Figure also shows the comparison of different MFR case to observe the effect of coolant amount to the secondary flow field. All cases have been compared with a baseline condition (no leakage case). For baseline condition, losses at blade downstream are significantly influenced by blade wake and another two loss cores which are located at  $y/p=0.5$ ,  $z/s=0.15$  and close to endwall,  $y/p=0.65$ , respectively. Based on the vorticity contour, first core can be considered is associated with the passage vortex which is rotating in anti-clockwise direction close to the blade suction side while the second core is associated with interaction between wall boundary layer, wake profile and corner vortex coming from upstream. The positive vorticity rotating in clockwise direction over the passage vortex demonstrates the counter vortex whereas the small blue region rotating in opposite direction probably the corner vortex coming from blade pressure side. The effect of the upstream leakage ejection can be observed in (b), (c) and (d) for MFR=1.0%, MFR=1.5% and MFR=2.1% respectively. Upstream leakage ejection obviously affected the flow field near the endwall region as shown in figures. The shape of first core seems to be changed and moved toward midspan. Furthermore, as the MFR increases, the center of this core became slightly higher in span direction. This phenomenon might be due to the increased strength of the passage vortex as the MFR being increased and consequently force the first core to move upward. The increase strength of



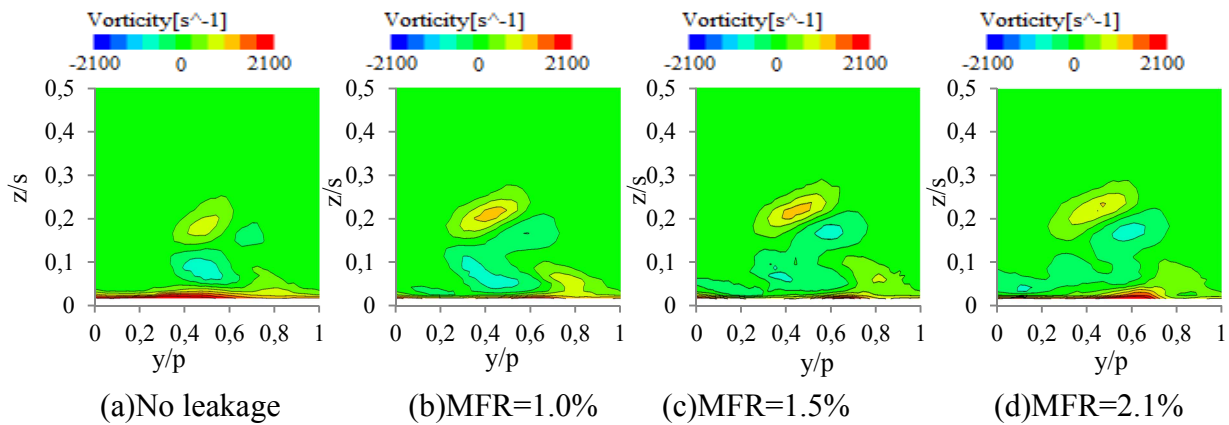
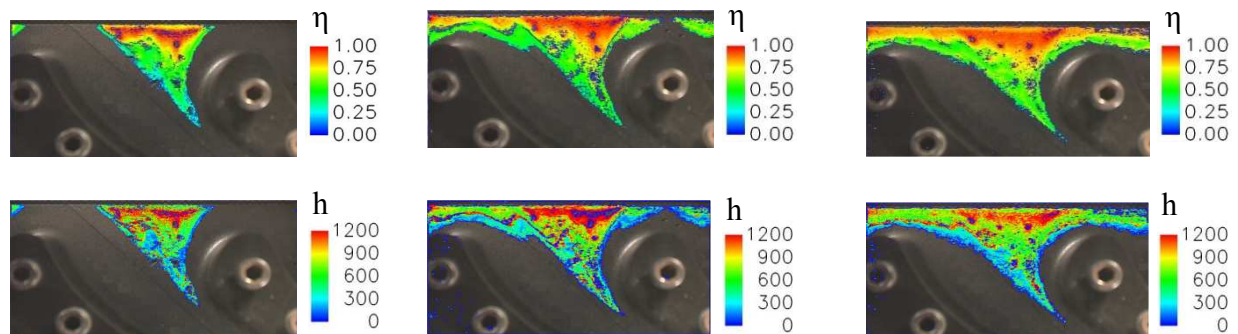


Fig. 2 Total pressure loss and vorticity for each case

passage vortex can be seen by the presence of vortical structures near the endwall presented by these secondary velocity vector superimposed. As the MFR increased, the center of vortical structures slightly shifted to the left side and moved away from blade SS. The second loss core also presented a significant changes where its spread the region radially and MFR=2.1% became the highest region compared to others. Figures also indicate that upstream leakage ejection not only effected the existing loss cores, but also influenced the new generation of loss core (third core) just below the first core for leakage ejection case with an increase trend with a higher MFR. Vorticity contours indicate that the passage vortex tends to merge with the corner vortex and produced a wider region of anticlockwise direction vorticity for all cases of ejection. By the increasing of MFR, the region of this vorticity spread in pitch direction and this could be consider as a reason the widest loss region was obtained in MFR=2.1%.

**Film Cooling Performance** Fig. 3 presents contours of measured film effectiveness (top) and heat transfer coefficient (bottom) on the endwall for 3MFR cases which were used in aerodynamics measurements. These contours indicate that the increase in MFR of the leakage flow from 1.0% to 2.1% enlarged the coverage of the leakage flow on the upstream portion of the endwall. For MFR=1.0% case, due to the higher pressure in stagnation region near the blade leading edge prevented the air from the plenum chamber to be ejected into mainstream and finally causes the uncovered areas by leakage flow. In contrast, when MFR increased to 1.5%, the secondary air might be considered have enough momentum to penetrate into the mainstream includes the stagnation region and presented a wider film coverage compared to 1.0% case. However, there are no dramatically changes in film coverage obtained when increasing MFR from 1.5% to 2.1%. Based on the results obtained, it could be considered that the film coverage is strongly influenced by the secondary flow on the endwall as significantly exhibit by the film effectiveness contour the traces of the horseshoe vortex at the blade leading edge. Those vortical structures prevented the leakage flow, which could be regarded as cooling air, from reaching the root section of the leading edge and the pressure side of the vane.



(a) MFR=1.0% (b) MFR=1.5% (c) MFR=2.1%  
Fig. 3 Film cooling effectiveness and heat transfer coefficient for each case

## Conclusions

The investigation of aero-thermal performance on turbine cascade endwall cooling by the influenced of upstream leakage flow have been done by measurements. Upstream leakage ejection obviously effected the secondary flow field. Ejected leakage flows caused the presence of additional losses region close to the endwall at blade suction side. As the MFR increases, this loss region became wider due to the increase strength of vortical structures near the endwall. This was also proved by the merging of the vorticity region to generate a wider vortical structure at higher MFR and contributed to the extra losses. Furthermore, the shape and position of first loss core were changed and moved towards midspan. The same phenomenon to the second loss core which is close to endwall, its increased the region radially up to 30% for MFR=2.1% compared to baseline condition. For the film cooling studies, MFR=1.5% illustrated significantly increase of film coverage compared to 1.0% case but only a slightly enlarged in coverage when increasing MFR to 2.1%. Based on heat transfer measurement, it was indicated that the film cooling effectiveness and heat transfer coefficient contour was strongly influenced by the secondary flow on the endwall.

## References

- [1] Blair, M.F., 1974, "An Experimental Study of Heat Transfer and Film Cooling on Large-Scale Turbine Endwalls", *ASME Journal of Heat Transfer*, 96, pp. 524-529.
- [2] Langston, L. S., Nice, M. L. and Hooper, R. M.; 1977 "Three-Dimensional Flow Within a Turbine Cascade Passage", *ASME Paper No. 76-GT-50, ASME Journal of Engineering for Power, Vol. 99, pp. 21-28.*
- [3] Takeishi, K., Matsuura, M., Aoki, S. and Sato, T.; 1990 "An Experimental Study of Heat Transfer and Film Cooling on Low Aspect Ratio Turbine Nozzles", *ASME Paper No. 89-GT-187, ASME Journal of Turbomachinery, Vol. 112, pp. 488-496.*
- [4] Wang, H. P., Olson, S. J., Goldstein, R. J. and Eckert, E. R. G.; 1995 "Flow Visualisation in a Linear Turbine Cascade of High Performance Turbine Blades", *ASME Paper No. 95-GT-7, Texas.*
- [5] Kost, F., and Nicklas, M., 2001. "Film-Cooled Turbine Endwall in a Transonic Flow Field: Part I - Aerodynamic Measurements," *ASME J Turbomach* 123, pp. 709–719.
- [6] Kost, F., and Mullaert, A., 2006. "Migration of Film-Coolant from Slot and Hole Ejection at a Turbine Vane Endwall". *GT2006-90355*
- [7] Papa, M., Srinivisan, V., Goldstein, R.j., 2010, "Film Cooling Effect of Rotor-Stator Purge Flow on Endwall Heat/Mass Transfer", *ASME Paper GT2010-23178.*
- [8] Funazaki, K., 2000, "Discussion on Accuracy of Transient Heat Transfer Measurement by Use of Thermochromic Liquid Crystal," *Journal of the Gas Turbine Society of Japan, Vol. 28, pp. 397-404.*

**Mechanical and Electrical Technology IV**

10.4028/www.scientific.net/AMM.229-231

**Aero-Thermal Performance of Purge Flow in Turbine Cascade Endwall Cooling**

10.4028/www.scientific.net/AMM.229-231.737